STUDIA UBB CHEMIA, LXXI, 2, 2026 (p. 189-208)
(RECOMMENDED CITATION)
DOI:10.24193/subbchem.2026.2.10

BEYOND THE SALINITY GRADIENT ENERGY HARVESTING

Cristiana-Nicoleta FUICU[a], Nicolae VASZILCSIN[b,c], Mircea-Laurențiu DAN[a], Delia-Andrada DUCA[a,*]

ABSTRACT. Recently, salinity gradient energy – known as blue energy – has sparked the interest of researchers in identifying a new source of renewable energy, available at the contact between river water and seawater. In this paper, which is a mini-review of the salinity gradient energy harvesting, the appreciable potential of this energy source is emphasized by calculating the thermodynamic effect of mixing a water of high salinity, which simulates seawater, with water of low salinity, characteristic of rivers. Unfortunately, this potential of salinity gradient energy is difficult to exploit due to technical limitations. In such circumstances, the seawater-river water system was approached as an electrochemical thermodynamic system, at the interface of which an electric potential difference occurs. In the simplest case, this is a diffusion potential, evaluated based on Henderson equation. The value of the diffusion potential is low (about 20 mV) because the interface between these two media is crossed by both cations and anions. If, however, the two media of different salinity are separated by an ion exchange membrane, there is a much larger potential difference between them (about 100 mV), called membrane potential, which can be capitalized using a concentration cell. Moreover, the main methods applied so far for the recovery of the salinity gradient energy are highlighted: pressure retarded osmosis, reverse electrodialysis and capacitive mixing methods.

Keywords: *diffusion potential, Henderson relationship, membrane potential, reverse electrodialysis, pressure retarded osmosis, blue energy, capacitive mixing method.*

[a] *Faculty of Chemical Engineering, Biotechnologies and Environmental Protection, University Politehnica Timisoara, 300223 Timisoara, Romania.*
[b] *Technical Sciences Academy of Romania, Bd. Dacia 26, 010414 Bucuresti, Romania.*
[c] *Research Institute for Renewable Energies, University Politehnica Timisoara, Piata Victoriei 2, 300006 Timisoara, Romania.*
[*] *Corresponding author: delia.duca@upt.ro*

INTRODUCTION

Over the past decades, especially after the Paris Agreement in 2015, signed by 195 states, research on renewable energy resources has been enhanced to reduce greenhouse gas emissions and maintain the increase in the global average temperature up to +2°C compared to the pre-industrial period [1-3]. Moreover, the United Nations Climate Conference COP29 (Baku 2024) recommended increasing efforts to protect the environment and mitigate climate change by imposing a +1.5 C° limit on the average temperature increase [4]. The constant interest in hydro, solar, wind, biomass renewable sources, as well as thermal water energy, has been followed by recent research for the use of low energy density sources, difficult to capitalize at commercial level, such as salinity gradient energy (SGE) [5-9].

In principle, SGE is the energy obtained by mixing two saline aqueous solutions, which differ in the concentration of the components. The Gibbs free energy change of mixing ΔG_{mix} can be calculated using the relation (1) [10-12].

$$\Delta G_{mix} = \nu RT \sum x_i ln x_i \quad (1)$$

where n is the number of chemical species (ionic species, in the case of electrolyte solutions), R – the universal gas constant, T – the thermodynamic temperature, x_i – the molar fraction of the chemical species i.

The idea of capitalizing the SGE has been launched as early as the middle of the last century by R. E. Pattle, who stated: "*when a river mixes with the sea, free energy equal to that obtainable from a water fall 680 ft. high is lost*" [13]. This remark of R. E. Pattle sparked the imagination of researchers who were probably already seeing the waters of the Amazon, with a flow of 200,000 $m^3\ s^{-1}$, passing through generators of electricity from a height equivalent to 207 m (680 ft.), before pouring into the Atlantic Ocean, thus ensuring the energy needs of all South America. Unfortunately, the possibilities offered by thermodynamics cannot always be fully exploited due to technical limitations.

In order to rigorously evaluate the energy available for the mixing of seawater and river water, equation (1) has been customized for the case of concentrated and diluted sodium chloride solutions (2) [14].

$$\Delta G_{mix} = 2RT[(n_c + n_d) ln x_{mix} - n_c ln x_c - n_d ln x_d] \quad (2)$$

where n_c and n_d are the number of moles of NaCl in the concentrated solution, respectively diluted, x_c, x_d and x_{mix} – the molar fractions of NaCl in the concentrated, diluted solution, respectively in the mixture of the two solutions. Factor 2 is due to the fact that NaCl is dissociated into the two ionic species Na^+ and Cl^-.

By replacing the molar fractions with the respective molar concentrations, the relationship (3) is obtained [14].

$$\Delta G_{mix} = -2RT\left[V_c c_c ln\frac{c_c}{c_{mix}} + V_d c_d ln\frac{c_d}{c_{mix}}\right] \quad (3)$$

where V_c and V_d are the volume of concentrated solution, respectively diluted, L; c_c, c_d and c_{mix} – the molar concentrations of NaCl in the concentrated, diluted and mixed solution, mol L^{-1}.

When mixing 1 L of 3.5% NaCl solution (0.6 mol L^{-1}), which simulates seawater, with 1 L of dilute NaCl solution (0.01 mol L^{-1}), which simulates river water, 2 L of 0.305 mol L^{-1} NaCl solution is obtained.

Under these conditions: $V_c = V_d = 1$ L; $c_c = 0.6$ mol L^{-1}; $c_d = 0.01$ mol L^{-1}; $c_{mix} = 0.305$ mol L^{-1}. The Gibbs free energy value will be:

$$\Delta G_{mix} = -2 \times 8.314 \times 298\left[1 \times 0.6ln\frac{0.6}{0.305} + 1 \times 0.01ln\frac{0.01}{0.305}\right] = -1842 \text{ J}$$

Therefore, for 1 L of seawater-river water mixture, an energy of 921 J is obtained, which means that the available energy is equivalent to the potential energy of a 1 L of mixture of the two solutions at a height of about 92 m. The value obtained is much lower than the one reported by R. E. Pattle (207 m), because in the evaluation of Gibbs free energy change the salinity of river water is taken into account and the obtained value is referred to 1 L of seawater – river water mixture.

The above evaluations of the SGE consider that the seawater-river water mixture is a thermodynamic system for which the available energy is given by ΔG_{mix}, without taking into account the fact that the interface between the two media is crossed by ionic species that have different mobilities. Under these circumstances, there is an electric potential difference between the two solutions, called diffusion potential, which can be harnessed from an energetic point of view.

DIFFUSION POTENTIAL

Let us consider two solutions 1 and 2 in contact, which contain the ionic species $X_1^{z_1}$, $X_2^{z_2}$ … $X_n^{z_n}$ at molar concentrations c_{11}, c_{21}, …, c_{n1}, in solution 1, respectively c_{12}, c_{22}, …, c_{n2}, in solution 2, z_i being the charge of X_i ion (Figure 1). When the solutions are in contact, both phases are electrically neutral, which means that $\sum_i z_i c_{i1} = 0$ şi $\sum_i z_i c_{i2} = 0$.

Since, the ionic species in the two solutions have different diffusion coefficients and implicit mobilities, under the influence of the concentration gradients between the two solutions, the ionic species will diffuse at different

rates, which will lead to the development of a potential difference, known as the diffusion potential Dϕ_d. It can be calculated using Henderson general equation (4) [15-17].

$$\Delta\phi_d = \phi_1 - \phi_2 = \frac{\sum_i \frac{u_i}{z_i}(c_{i2}-c_{i1})}{\sum_i u_i(c_{i2}-c_{i1})} \cdot \frac{RT}{F} ln \frac{\sum_i u_i \cdot c_{i2}}{\sum_i u_i \cdot c_{i1}} \quad (4)$$

where ϕ_1 is the potential of the solution 1, ϕ_2 – the potential of the solution 2, u_i – mobility of the ionic species *i*.

Diffusion potential $\Delta\phi_d$ is not a constant value, it decreases continuously as the concentrations in the solutions in contact are equalized, and when the equilibrium is reached $\Delta\phi_d = 0$.

For two solutions of the same electrolyte at different concentrations, in contact, the diffusion potential is given by the relationship (5).

$$\Delta\phi_d = \phi_1 - \phi_2 = \frac{\frac{u_1}{z_1}(c_{12}-c_{11})+\frac{u_2}{z_2}(c_{22}-c_{21})}{u_1(c_{12}-c_{11})+u_2(c_{22}-c_{21})} \cdot \frac{RT}{F} ln \frac{u_1 \cdot c_{12}+u_2 \cdot c_{22}}{u_1 \cdot c_{11}+u_2 \cdot c_{21}} \quad (5)$$

For a z–z valent electrolyte, completely dissociated into ions X_1^{z+} and X_2^{z-}, for which the concentrations of the two ionic species in the same solution are equal to each other ($c_{11} = c_{12} = c_1$ and $c_{21} = c_{22} = c_2$, the equation (5) is simplified in the form given to the relationship (6).

$$\Delta\phi_d = \phi_1 - \phi_2 = \frac{u_c - u_a}{u_c + u_a} \cdot \frac{RT}{zF} ln \frac{c_2}{c_1} \quad (6)$$

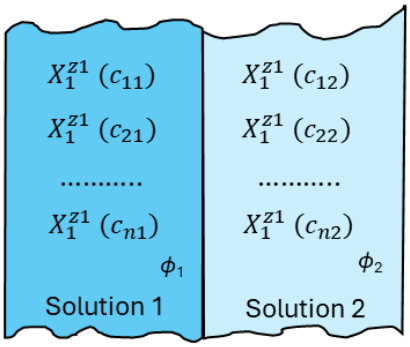

Figure 1. Diffusion potential at the interface between solutions 1 and 2.

Let us take as an example two sodium chloride solutions, one with a concentration of c_1 = 0.6 mol L^{-1} (phase 1), similar to the concentration of seawater, and one with a reduced salinity of c_2 = 0.01 mol L^{-1} sodium chloride (phase 2), which simulates river water.

The ionic mobility for Na^+ is u_{Na^+} = 5.19·10^{-8} m^2 V^{-1} s^{-1}, and the one for Cl^- is u_{Cl^-} = 7.92·10^{-8} m^2 V^{-1} s^{-1} [18]. Whereas $u_{Na^+} < u_{Cl^-}$, the diffusion of Cl^- ions from the concentrated solution to the diluted solution will be faster than that of Na^+ ions. Consequently, the diluted solution becomes enriched in negative charges, whereas the more concentrated solution exhibits an excess of positive charges. Using the relation (3), for the diffusion potential, the value $\Delta\phi_d = 22\ \mathrm{mV}$ is obtained.

More accurate values of diffusion potential can be obtained if the average activities of the ionic species $a = f_{\pm} \times c$ are involved instead of concentrations. For 0.6 mol L^{-1} NaCl solution, the average activity coefficient is $f_{\pm 1}$ = 0.675, and for 0.01 mol L^{-1} NaCl solution, $f_{\pm 2}$ = 0.902 [19]. Accordingly, for the diffusion potential, the value $\Delta\phi_d$ = 20 mV has been obtained.

Since the difference between the two values is insignificant, we will still use concentrations instead of activities and ionic mobilities at infinite dilution instead of real mobilities.

Certainly, both seawater and river water have a much more complicated composition. An approximate composition of seawater and the water of an arbitrary river is given in Table 1.

Table 1. Ionic mobilities [18,20] and the average composition of seawater [21] and river water

Ionic species	Ionic mobility $u^o \cdot 10^8$ [m^2 s^{-1} V^{-1}]	Molar mass [g mol^{-1}]	Concentration in seawater		Concentration in river water	
			[g L^{-1}]	[mol L^{-1}]	[g L^{-1}]	[mol L^{-1}]
Cl^-	7.92	35.45	19.162	c_{11}=0.5405	0.070	c_{12}=0.001975
Na^+	5.19	22.99	10.679	c_{21}=0.4645	0.070	c_{22}=0.003045
Mg^{2+}	4.18	24.31	1.278	c_{31}=0.0526	0.020	c_{32}=0.000823
SO_4^{2-}	8.29	96.06	2.680	c_{41}=0.0278	0.100	c_{42}=0.001041
Ca^{2+}	6.16	40.08	0.4096	c_{51}=0.0010	0.080	c_{52}=0.001996
K^+	7.62	39.10	0.3953	c_{61}=0.0101	0.005	c_{62}=0.000128
HCO_3^-	4.59	61.02	0.0276	c_{71}=.00045	0.150	c_{72}=0.002458
Br^-	8.10	79.90	0.0663	c_{81}=.00083	0	c_{82}=0
NO_3^-	7.40	62.00	0	c_{91}= 0	0.020	c_{92}=0.000323

It is easy to see that the diffusion potential is a non-equilibrium potential, since the ionic species in the more concentrated solution will continuously pass into the dilute solution until the concentrations are equalized, when the diffusion potential becomes zero. On the other hand, the

equalization of concentrations can be achieved not only as a result of a concentration gradient, but also by convection, because of a density, pressure or temperature gradient, a phenomenon that accelerates the uniformity of the ionic concentrations in the solutions in contact. To avoid convection phenomena, the two solutions can be separated by non-selective diaphragms, which allow the passage of all ionic species present in the electrolyte solutions.

An efficient exploitation of the energy potential at the saline/ freshwater interface can be achieved by using a selective separator of ionic species between in solutions in contact, e.g., a cation- or anion exchange membrane.

Consider the case where the two solutions of NaCl 0.6 mol L^{-1} (solution 1) and 0.01 mol L^{-1} (solution 2) are separated by a cation exchange membrane (CEM), e.g., Nafion (Figure 2) [22, 23].

Under the action of the concentration gradient between the two electrolyte solutions, only Na^+ ions can cross the membrane. The equilibrium state will be reached when the electrochemical potentials of the Na^+ ions in both solutions become equal (7).

$$\bar{\mu}_{Na^+(1)} = \bar{\mu}_{Na^+(2)} \tag{7}$$

where $\bar{\mu}_{Na^+(1)}$ şi $\bar{\mu}_{Na^+(2)}$ are the electrochemical potentials of Na^+ ions in solutions 1 and 2.

By explicitly expressing Na^+ ions electrochemical potentials, the relation (8) is obtained.

$$\mu^o_{Na^+} + RTlgc_{Na^+(1)} + F\phi_1 = \mu^o_{Na^+} + RTlgc_{Na^+(2)} + F\phi_2 \tag{8}$$

Therefore, the potential that arises between the two solutions separated by the cationic membrane, called the membrane potential $\Delta\phi_M$, will be given by the relation (9).

$$\Delta\phi_M = \phi_2 - \phi_1 = \frac{RT}{F} ln \frac{c_{Na^+(1)}}{c_{Na^+(2)}} \tag{9}$$

Numerical value for concentrations $c_{Na^+(1)}$= 0.6 mol L^{-1} and $c_{Na^+(2)}$ = 0.01 mol L^{-1}, is $\Delta\phi_M = 0.105$ V, significantly higher than the diffusion potential $\Delta\phi_d$.

If ionic mean activities are used instead of concentrations, the value of $\Delta\phi_M$ = 98 mV is obtained, close to that obtained using the concentrations of ionic species.

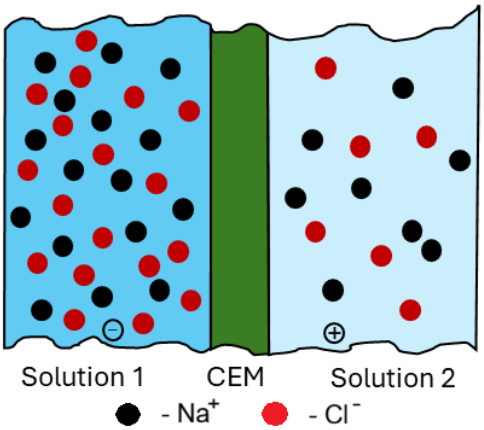

Figure 2. The emergence of the membrane potential across the two interfaces of the Nafion (CEM).

If an anion exchange membrane is used, only the Cl^- ions will diffuse through the membrane until electrochemical equilibrium is reached, when the electrochemical potential of the chloride ions in solution 1 will become equal to that in solution 2. Under these conditions, the expression of the membrane potential in this case is given by the relation (10) [22].

$$\Delta\phi_M = \phi_1 - \phi_2 = \frac{RT}{F} ln \frac{c_{Cl^-(1)}}{c_{Cl^-(2)}} \quad (10)$$

Measurement of the diffusion or membrane potential is possible by inserting two inert electrodes into the two electrolyte solutions. The electrochemical cell thus realized is known as the concentration cell.

CONCENTRATION CELLS

By introducing two inert metals into the two electrolyte solutions in contact, an electrochemical concentration cell is achieved. If the same electrochemical equilibrium is established at the two electrodes, then the electromotive force of the concentration cell will be equal to the diffusion potential or the membrane potential. Figure 3 shows a concentration cell with the electrochemical chain Pt (H_2)/H_2(g), H^+(aq), NaCl(c_1)//NaCl(c_2), H^+(aq), H_2(g)/Pt(H_2), in which the solutions are separated by a cation exchange membrane [23], and Figure 4 shows the profile of the Galvani potential (ϕ) along the electrochemical chain of the cell.

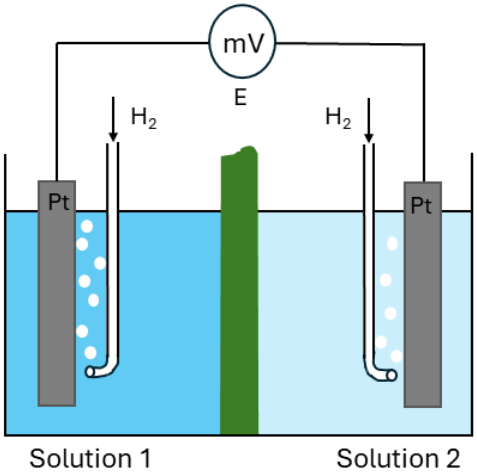

Figure 3. Concentration cell Pt (H_2)/H_2(g), H^+(aq), NaCl(c_1)//NaCl(c_2), H^+(aq), H_2(g)/Pt(H_2).

From the electrochemical chain of the concentration cell, it can be seen that the two electrodes are hydrogen electrodes whose absolute potential is given by the relation (11).

$$\Delta\phi_{eq} = \Delta\phi^{o}_{H_2/H^+} + \frac{RT}{F} ln \frac{a_{H^+}}{\sqrt{p_{H_2}}} \quad (11)$$

where $\Delta\phi^{o}_{H_2/H^+}$ is the absolute potential of the standard hydrogen electrode, p_{H_2}- hydrogen partial pressure, a_{H^+}- hydronium ion activity.

Since the hydrogen electrodes are identical, at the two Pt - electrolyte solution interfaces, the Galvani potential drops are identical (12) as shown in Figure 4.

$$\phi_{Pt1} - \phi_{S1} = \phi_{Pt2} - \phi_{S2} \quad (12)$$

According to Figure 4, the electromotive force, measured with an electronic voltmeter having high input impedance, in order do not allow a current during the measurement, is given the algebraic sum of the potential drops in the electrochemical chain (13).

$$E = \phi_{Pt1} - \phi_{S1} - \Delta\phi_M + \phi_{S2} - \phi_{Pt2} \quad (13)$$

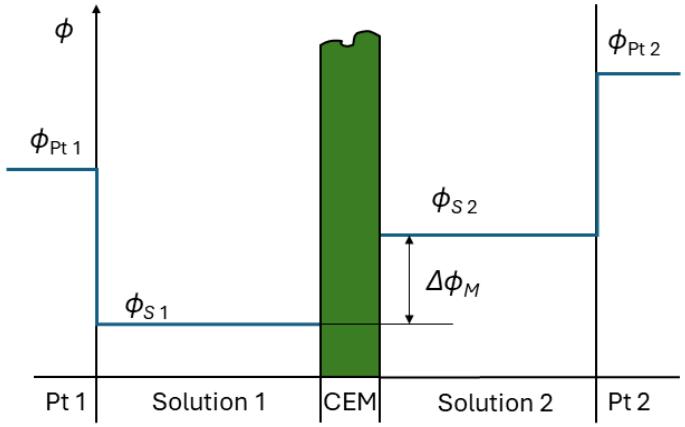

Figure 4. Potential Galvani profile along the electrochemical system.

Therefore, the membrane potential is numerically equal to the value of the cell electromotive force with opposite sign (14).

$$\Delta\phi_M = -E \tag{14}$$

As a rule, such concentration cells are not used as electrochemical power sources, owing to their low energy density and significant internal resistance. Their practical relevance lies primarily in potentiometric measurement for evaluating the electrolyte activity in solutions. The most well-known application is the glass electrode, a selective-ion electrode used to determine the activity of hydronium ions in electrolyte solutions. Ion-selective electrodes have also been developed for the quantitative determination of anionic or cationic species in aqueous solutions [24-28].

Modified concentration cells can be used to convert salinity gradient energy into electrical energy. In such systems, when current flows through the external circuit, reduction takes place at the cathode and oxidation at the anode. Equations (9) and (10), used to evaluate the membrane potential $\Delta\phi_d$, provide the maximum electromotive force *E*, corresponding to the thermodynamic equilibrium state. The value of *E* decreases over time as the concentration gradient between the two solutions diminishes. Under dynamic operating conditions, the actual cell voltage is lower than the *E* because of polarization effects.

BLUE ENERGY HARVESTING

The most important technical variants for the valorisation of SGE are pressure retarded osmosis (PRO), reverse electrodialysis (RED) and capacitive mixing (CapMix) [29-32].

Pressure retarded osmosis is a widely studied technology for capturing SGE, originating from pioneering research of S. Loeb et al. in 1976. They have used a semi-permeable membrane between seawater and river water [33]. This allows the passage of water molecules from river water (diluted) to seawater (concentrated), creating a pressure difference due to the osmosis phenomenon, which is converted into electricity by means of a turbine (Figure 5) [7,34,35]. At equilibrium, the pressure difference becomes equal to the osmotic pressure.

One of the most important components of the PRO system is the semi-permeable membrane, which must permit the passage of water molecules while effectively restricting the transfer of ionic species. Consequently, membranes employed in PRO technology are typically composite structures integrated into a rigid support in order to withstand the pressure difference between the seawater and river water compartments [36,37]. Successful semi-permeable membranes have proven to be those that have a polyamide or polyamide-polyethylene composites as a selective layer. Polydopamine is also a promising polymer, as it contains both nucleophilic and electrophilic groups in its structure [38].

For PRO technology, various values of power densities have been reported: 2.56 W m^{-2} [39], 0.7 – 1.2 W m^{-2} [40], but also exceedingly high values, difficult to achieve under normal conditions: 38 W m^{-2} [41].

Reverse electrodialysis is based on bringing seawater and river water into contact by means of two ion-selective membranes: an anion exchange membrane and a cation exchange one (Figure 6). Seawater flows between the two membranes, while river water circulates in the outer compartments. The anion exchange membrane will allow the passage of anions from seawater to river water in the left compartment, which will acquire an excess of negative charges. At the same time, the cation exchange membrane will allow cations to pass from seawater to river water, which will thus have an excess of positive electrical charges. Therefore, if inert electrodes are placed into the two extreme compartments, an electromotive force is generated between them, thus creating an electrochemical power source that converts SGE into electricity [42].

Basically, a cell stack is used to transform the SGE into electricity in which the anion exchange membranes alternate with the cation exchange ones, so that the potential difference at the ends of the cell is increased (Figure 7) [43,44]. J. Veermana et al. realized a stack of 50 elementary cells, supplied with solutions simulating seawater and river water, except for the electrode compartments fed with potassium hexacyanoferrate(II) and potassium hexacyanoferrate(III) solution. In these circumstances, electricity generation occurs via the oxidation of hexacyanoferrate(II) to hexacyanoferrate(III) at the anode, and the reverse reduction reaction at the cathode. Titanium

meshes coated with ruthenium and iridium oxides layers have been used as electrodes [45]. Other authors have reported the use of platinum or iridium films deposited on titanium mesh [12].

In general, the ion-exchange membranes employed in the RED technique are similar to commercially available membranes used in electrolyzers and fuel cells. P. Długołęcki et al. investigated Tokuyama Corporation Neosepta membranes and Asahi Glass Co. Selemion membranes in RED cells. The Neosepta CMX and Selemion CMV membranes are cation-exchange membranes based on a styrene–divinylbenzene copolymer reinforced with polyvinyl chloride, containing sulfonate groups $-SO_3^-$ as fixed ionic groups. In contrast, the Neosepta AMX and Selemion APS membranes are anion-exchange membranes containing quaternary ammonium groups $-NR_3^+$ as fixed ionic groups. In addition, membranes produced by FUMATECH (Fumasep) and MEGA (Ralex) have also been reported in the literature [42]. J. W. Post et al. established several requirements that membranes used in RED must satisfy in order to achieve acceptable energy efficiency: permselectivity > 95%; electrical resistance < 3 Ω cm²; chemical stability with a lifetime > 5 years; sufficient mechanical strength for stack construction; and a cost below 2 €/m² [11]. A rigorous comparison of the different types of cation- and anion exchange membranes used in RED was conducted by Jaewon Jang et al. [46].

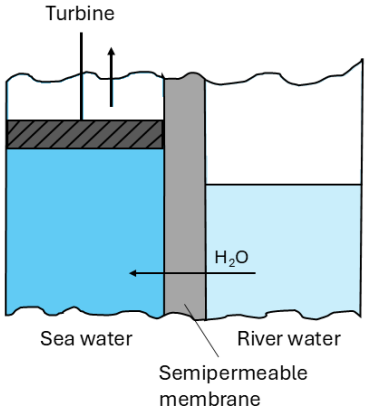

Figure 5. PRO principle.

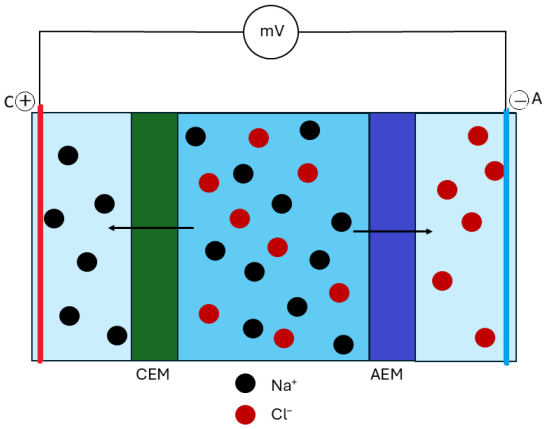

Figure 6. RED principle.

The maximum power density that can theoretically be achieved in RED technology is 6 W m^{-2}, but considering the limitations introduced by the selectivity of the membranes, as well as their specific conductivity, practical values of the power density of up to 2.4 W m^{-2} [47].

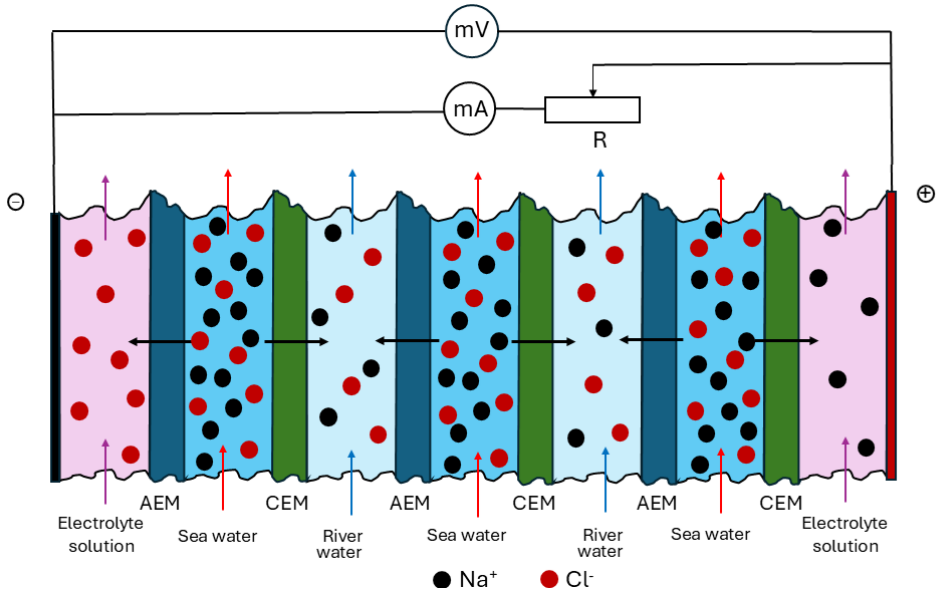

Figure 7. RED cell stack.

A simplified variant of RED is *nanopore power generation* (NPG), which employs a single separator between concentrated saline and diluted solution, thus reducing energy converter costs (Figure 8) [48]. As interphase separators, nanotubes with atoms or groups of atoms carrying electric charges are used, which reject selectively the diffusion of ions with electric charges of the same sign.

As an interphase separator, the use of boron nitride nanotubes has been proposed. Due to the partial hydration of boron nitride, according to the reaction (15), immobilized negative charges are generated into the nanotubes.

$$BN + 2H_2O \rightleftarrows HNBO^- + H_3O^+ \quad (15)$$

Consequently, an interphase separator based on boron nitride nanotubes allows the passage of cations but prevents the access of anions [49]. Recently, membranes have been made based on alumina nanotubes [50], molybdenum disulfide [51,52] or silicon nitride [53,54].

Capacitive mixing method (CapMix) is a reversible electrical energy storage system based on the electric double-layer capacitance at the interfaces between electronic and ionic conductors. In practice, a supercapacitor is used, consisting of an electrolytic cell equipped with inert electrodes possessing a very high specific surface area. Typically, the electrodes are made of activated

carbon, which provides high electrical capacitance through the specific adsorption of ionic species from the solution in contact with the electrode surface (Figure 9) [35,55,56].

In the first stage of capacitor charging, the electrochemical cell is filled with seawater. At the activated carbon–seawater interface A, connected to the positive terminal of the external power source, Cl^- ions are adsorbed, leading to an increase of the electric double-layer (EDL) capacitance at interface A. The extent of charge separation increases with the concentration of Cl^- ions in the solution. The negative plate of the EDL at interface A is located on the electrode surface, whereas the positive plate is situated in the electrolyte solution.

Similarly, at the activated carbon–seawater interface B, connected to the negative terminal of the power source, Na^+ ions are adsorbed, resulting in an increase in the EDL capacitance at interface B. In this case, the positive plate of the EDL is formed on the activated carbon surface, while the negative plate is located in the solution. Consequently, the electrochemical cell can be regarded as a system of two capacitors connected in series, where the terminal voltage is equal to the sum of the absolute values of the potential drops across the two EDLs.

In the second stage, during the discharge of the capacitor, the seawater in the cell is replaced with river water. In this manner, by replacing the concentrated solution with a dilute one, the EDL thickness at both interfaces (A and B) increases, leading to a rise in the voltage at the cell's terminals. In fact, the use of the dilute solution allows for an advanced discharge of the two EDLs, given that the electrical permittivity of the two solutions does not change significantly [54, 57].

An advanced configuration of CapMix separates the two activated carbon electrodes with a cation exchange membrane and an anion exchange membrane, respectively (Figure 10) [58–61].

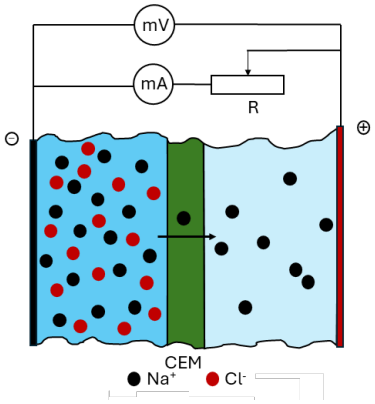

Figure 8. NPG principle.

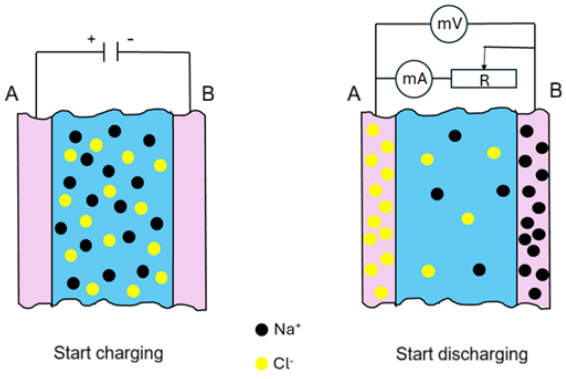

Figure 9. CapMix principle.

In this way, during the charging cycle, Na^+ ions spontaneously cross the cation exchange membrane and are adsorbed into the surface of the activated carbon, while Cl^- ions cross the anion exchange membrane and are adsorbed onto the surface of the opposite electrode. Since the two charging processes of the EDL at interfaces A and B are spontaneous, it is not necessary to polarize the electrodes using an external source. Equilibrium at the electronic conductor – ionic conductor interface A is established when the electrochemical potential of the adsorbed Na^+ ions becomes equal to their electrochemical potential in the seawater. Similarly, equilibrium at interface B is reached when the electrochemical potential of the adsorbed Cl^- ions equals that of the Cl^- ions in the seawater. As a result, a charge difference is generated between the two electrodes, which can subsequently be converted into electrical energy during the second discharge stage, when a dilute solution is passed between the electrodes.

Since the two charging processes of the EDL at interfaces A and B are spontaneous, it is not necessary to polarize the electrodes using an external source. Equilibrium at the electronic conductor – ionic conductor interface A is established when the electrochemical potential of the adsorbed Na^+ ions becomes equal to their electrochemical potential in the seawater. Similarly, equilibrium at interface B is reached when the electrochemical potential of the adsorbed Cl^- ions equals that of the Cl^- ions in the seawater. As a result, a charge difference is generated between the two electrodes, which can subsequently be converted into electrical energy during the second discharge stage, when a dilute solution is passed between the electrodes.

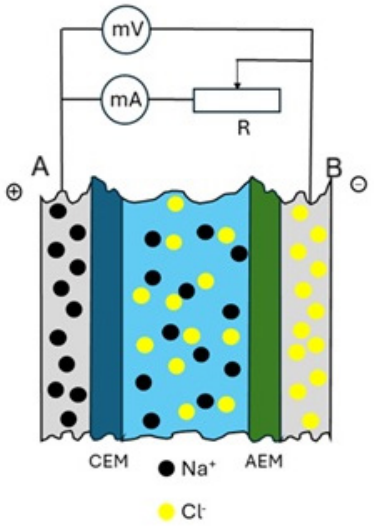

Figure 10. Advanced CapMix.

At the current level of research, the power density obtained by the CapMix technique is much lower than in the case of the PRO and RED methods. The most optimistic ratings for CapMix do not exceed 0.9 W m^{-2} [62,63]. On the other hand, the practical application of this technique has difficulties due to the membrane fouling and technical challenges of replacing seawater with river water in a short timeframe and without cross-dilution [35].

S. Sarp et al. have shown that PRO technology has some advantages over other SGE conversion methods, such as higher power density, as well as the possibility to use membranes from water desalination plants [64]. In 2009, the SINTEF research institute put into operation, in Tofte (Norway), an experimental facility to allow obtaining the necessary data for the application of PRO technology on a commercial scale [65]. Recently, in Japan, at Fukuoka, a PRO facility was put into operation, which is set to generate about 880,000 kWh per year [66]. Since the efficiency of the PRO method is dependent on the salinity difference between the two solutions, the Fukuoka facility was coupled with the desalination plant, using the resulting brine as a concentrated solution. As disadvantages of PRO, the following can be mentioned: the necessity of a large salinity gradient, the sensitivity of the membranes to impurities presents in the used solutions, as well as the use of moving equipment - the turbine that converts SGE into electrical energy. The RED technique, although it is not yet applied at a commercial level, has the advantage of the possibility to capitalize on small salinity differences between the two solutions, without the necessity of using a turbine. Unfortunately, this process also has a series of disadvantages: the sensitivity and high costs of the membranes, to which are added the construction difficulties due to the high internal electrical resistance of the solutions in the cell compartments. The CapMix method has the advantage of using a simple cell design, as well as inexpensive carbon-based electrodes, but their reduced mechanical resistance is a challenge for researchers. Constructive versions without ion-exchange membranes, although economically advantageous, are not efficient from an energetic point of view.

CONCLUSIONS

SGE, known within the scientific community as *blue energy*, remains a major challenge for researchers in the field of renewable energies. In principle, SGE represents the energy obtained by mixing two saline solutions that differ in their component concentrations, with the available energy being determined by the variation in the Gibbs free energy of mixing ΔG_{mix}. R. E. Pattle was the first to suggest the concept of harvesting the salinity gradient

between seawater and river water. The Gibbs free energy of mixing for 1 L of 0.6 mol L^{-1} NaCl solution (simulating seawater) with 1 L of 0.01 mol L^{-1} NaCl solution (simulating river water) is 1842 J. This implies that upon mixing the two solutions, the temperature increases by approximately 0.2 K, a variation that is difficult to exploit using a thermal engine.

Harvesting this Gibbs free energy variation ΔG_{mix} can be achieved by separating the two solutions with a selective membrane, which allows the passage of water molecules while rejecting the solutes. Driven by osmotic pressure, water molecules flow from the dilute solution to the concentrated one, thereby creating a hydraulic head that drives a turbine connected to an electrical generator. This constitutes the operating principle of PRO (Pressure-Retarded Osmosis) for converting SGE into electricity.

Furthermore, the electrochemical route represents another technique for harvesting the Gibbs free energy variation ΔG_{mix}. Due to the differences in mobility between Na^+ and Cl^- ionic species, a diffusion potential arises between the two solutions, which can be calculated using the Henderson equation. For the two solutions under consideration, the diffusion potential is approximately 20 mV. Naturally, as the two solutions mix, the diffusion potential decreases, reaching zero when the concentrations equalize. To prevent the mixing of the solutions, they can be separated by an ion-exchange membrane. By inserting two inert electrodes into the two solutions, a concentration cell is realized, whose electromotive force is numerically equal to the membrane potential $\Delta\phi_M$.

In the case of the 0.6 mol L^{-1} and 0.01 mol L^{-1} NaCl solutions separated by a cation-exchange membrane, the initial electromotive force was approximately 100 mV. In practice, however, a cell stack is realized, in which the compartments are alternately separated by cation- and anion-exchange membranes, thereby yielding a significantly higher electromotive force. Since the electrodes within the electrode compartments are identical, noble metals in a hexacyanoferrate(II) / hexacyanoferrate(III) solution, the electromotive force is determined by the sum of all absolute membrane potentials. Nanotubes functionalized with charged atoms or functional groups, which repel the diffusion of co-ions (ions bearing charges of the same sign), can also be utilized as separators between the two solutions.

Another electrochemical process for SGE conversion is the capacitive mixing method, which is based on the electric double-layer capacitance at the electronic conductor–ionic conductor interface. In practice, this is implemented as a carbon-based electrode supercapacitor. Charging of the supercapacitor is accomplished by passing seawater through the capacitor plates, whereas its discharging is carried out using river water. If the capacitor plates are isolated with a cation-exchange membrane and an

anion-exchange membrane, respectively, the charging of the electric double-layer occurs spontaneously, requiring no external energy input.

The analysis conducted by Shihong Lin et al. [35] demonstrated that, currently, SGE is not yet competitive due to the following reasons: the energy density of the seawater–river water system is low; the conversion efficiency of SGE into other energy forms is reduced due to technical difficulties that limit the advanced conversion of SGE into useful work; the membranes utilized in SGE conversion are expensive and sensitive to impurities present in the water; and the activity of the electrodes degrades over time. Among SGE conversion technologies, PRO is the most advanced, having reached a commercial level through the commissioning of a facility in Fukuoka, Japan; this plant utilizes the brine resulting from a desalination facility, which is significantly more concentrated than standard seawater.

Moreover, the European Commission has notified in 2014 that the exploitation of "Blue energy" currently involves excessive costs, and overcoming this bottleneck requires additional public support to render SGE conversion techniques economically viable [60]. Achieving this objective necessitates further experimental research into SGE conversion, targeting the following goals: the development of active electrodes to minimize their polarization during electricity generation in the external circuit; the identification of membranes with high selectivity and low electrical resistivity; the design of cells with ultra-narrow compartments to reduce the voltage drop within the solution; and the assurance of an optimal hydrodynamic flow regime to maintain high salinity gradients between the solutions in contact.

ACKNOWLEDGEMENTS

The authors gratefully acknowledge the support of the Doctoral School of the University Politehnica Timişoara in the preparation of this paper.

REFERENCES

1. N. Yilmaz; K. Looby; A. Atmanli; *Int. J. Hydrogen Energy*, **2025**, *150*, 150133.
2. F. P. Pinheiro; D. M. Gomes; F. L. Tofoli; R. F. Sampaio; L. S. Melo; R. C. F. Gregory; D. Sgro; R. P. S. Leao; *Int. J. Hydrogen Energy*, **2025**, *97*, 690–707.
3. M. Akhtaruzzaman; A. K. Banerjee; S. Boubaker; *Energy Econ.*, **2025**, *145*, 108185.
4. B. Su; W. Dong; T. Jiang; Z. W. Kundzewicz; *Innov.*, **2025**, *8*, 100888.
5. D. Jina; Y. Jinb; *Chem. Eng. Res. Des.*, **2023**, *198*, 69–80.

6. X. Y. Yuan; W. B. Zhang; A. Batol; X. Y. Liu; N. S. Zhou; J. Zhou; J. Feng; J. H. Liu; X. J. Ma; *Chem. Eng. J.*, **2025**, *519*, 165103.
7. Z. Jia; B. Wang; S. Song; Y. Fan; *Renew. Sustain. Energy Rev.*, **2014**, *31*, 91–100.
8. D. Suárez-Alfonso; A. Ruiz-García; M. Khayet; *Renew. Energy*, **2026**, *256*, 124344.
9. P. Wang; Y. Liu; Y. Li; T. Tang; Q. Ren; *Energy*, **2024**, *313*, 133729.
10. K. Touati; G. Nouri; C. N. Mulligan; *J. Environ. Chem. Eng.*, **2025**, *13*,118490.
11. J. W. Post; C. H. Goeting; J. Valk; S. Goinga; J. Veerman; H. V. M. Hamelers; P. J. F. M. Hack; *Desalin. Water Treat.*, **2010**, *16*, 182–193.
12. R. A. Tufa; S. Pawlowski; J. Veerman; K. Bouzek; E. Fontananova; G. di Profio; S. Velizarov; J. G. Crespo; K. Nijmeijer; E. Curcio; *Appl. Energy*, **2018**, *225*, 290–331.
13. R. E. Pattle; *Nature*, **1954**, *174*, 660.
14. K. Watanabe; Y. Akiba; H. Ishidaira; H. Shima; *Desalination*, **2025**, *605*, 118706.
15. N. Bonciocat; *Electrochimie şi aplicaţii*, Editura Dacia Europa Nova, Timişoara, România, **1996**, pp. 87.
16. K. J. Vetter; *Electrochemical Kinetics: Theoretical Aspects*, Academic Press, New York, **1967**, pp. 48.
17. O. A. Petrii; G. A. Tsirlina; *Electrode potentials*. In Encyclopedia of Electrochemistry, 1st ed.; E. Gileadi, M. Urbakh Eds.; Wiley-VCH, Weinheim, Germany, **2002**; Volume 1, pp. 9.
18. L. Oniciu; E. Constantinescu; *Electrochimie şi coroziune*, Editura Didactică şi Pedagogică, Bucureşti, România, **1982**.
19. D. Dobos; *Electrochemical Data*, Elsevier Scientific, Amsterdam, Olanda, **1975**.
20. Y. D. Raka; R. Bock; H. Karoliussen; Ø. Wilhelmsen; O. S. Burheim; *Membranes*, **2021**, *11*, 135.
21. https://www.britannica.com/science/seawater
22. C. Gui; B. Liao; X. Zhang; Y. Wang; G. Ding; H. Huang; T. Ren; P. Liu; X. Hu; L. Huang; *Chem. Eng. Sci.*, **2026**, *320*, 122605.
23. R. W. Baker; *Membrane Technology and Applications*, McGraw Hill, New York, USA, **2000**.
24. G. Wilczek-Vera; J. H. Vera; *Fluid Phase Equilib.*, **2005**, *236*, 96–110.
25. P. Ocon; M. D. Reboiras; *Bioelectrochem. Bioenerg.*, **1987**, *17*, 489-501.
26. R. Stepak; *Anal. Chim. Acta*, **1987**, *203*, 79-83.
27. G. Scatchard; W. H. Orttung; *J. Colloid Interface Sci.*, **1966**, *22*, 12-18.
28. S. B. B. Solberg; M. Hammer; Ø. Wilhelmsen; S. Burheim; *Fluid Phase Equilib.*, **2024**, *586*, 114173.
29. G. Tan; S. Lu; J. Fan; G. Li; X. Zhu; *Electrochim. Acta*, **2019**, *322*, 134724.
30. M. Essalhi; A. H. Avci; F. Lipnizki; N. Tavajohi; *Renew. Energy*, **2023**, *215*, 118984.
31. K. Touati; G. Nouri; C. N. Mulligan; *J. Environ. Chem. Eng.*, **2025**, *13*, 118490.
32. X. Zhou; W. – B. Zhang; J. – J. Li; X. Bao; X. – W. Han; M. M. Theint; X. – J. Ma; *Energy Convers. Manag.*, **2022**, *255*, 115315.

33. S. Loeb; F. Van Hessen; D. Shahaf; *J. Membr. Sci.*, **1976**, *1*, 249-269.
34. J. Pan; W. Xu; Y. Zhang; Y. Ke; J. Dong; W. Li; L. Wang; B. Wang; B. Meng; Q. Zhou; F. Xia; *Nano Energy*, **2024**, *132*, 110412.
35. S. Lin; Z. Wang; L. Wang; M. Elimelech; *Joule*, **2024**, *8*, 334–343.
36. M. Sharma; P. P. Das; A. Chakraborty; M. K. Purkait; *Sustain. Energy Technol. Assess.*, **2022**, *49*, 101687.
37. J. T. Arena; K. K. Reimund; J. R. McCutcheon; *Desalination*, **2021**, *498*, 114804.
38. M. Malankowska; Z. Su; K. Karlsen; M. F. Buhl; H. Guo; L. S. Pedersen; M. Pinelo; *Chem. Eng. J.*, **2024**, *297*, 120221.
39. D. Suárez-Alfonso; A. Ruiz-García; M. Khayet; *Renew. Energy*, **2026**, *256*, 124344.
40. M. Sharma; P. P. Das; A. Chakraborty; M. K. Purkait; *Sustain. Energy Technol. Assess.*, **2022**, *49*, 101687.
41. A. Altaee; A. Cipolina; *Renew. Energy*, **2019**, *141*, 139-147.
42. P. Długołecki; K. Nymeijer; S. Metz; M. Wessling; *J. Membr. Sci.*, **2008**, *319*, 214–222.
43. Z. Y. Guo; W. Z. Cui; Z. Y. Ji; K. Tumba; J. Wang; L. J. Fu; Z. X. Zhang; J. Liu; Y. Y. Zhao; Z. D. Zhang; J. S. Yuan; *Desalination*, **2023**, *566*, 116900.
44. J. Veerman; M. Saakes; S. J. Metz; G. J. Harmsen; *J. Membr. Sci.*, **2009**, *327*, 136–144.
45. R. A. Tufa; S. Pawlowski; J. Veerman; K. Bouzek; E. Fontananova; G. di Profio; S. Velizarov; J. G. Crespo; K. Nijmeijer; E. Curcio; *Appl. Energy*, **2018**, *225*, 290–331.
46. J. Janga; Y. Kanga; J. H. Hanb; K. Janga; C. M. Kima; I. S. Kima, *Desalination*, **2020**, *491*, 114540.
47. Z. Wang; L. Wang; M. Elimelech; *Engineering*, **2022**, *9*, 51–60.
48. A. Siria; P. Poncharal; A. L. Biance; R. Fulcrand; X. Blasé; S. T. Purcell; L. Bocquet; *Nature*, **2013**, *494*, 455–458.
49. J. Wang; C. S. Law; K. N. Vu; S. Gunenthiran; K. Nielsch; A. D. Abell; A. Santos; *Chem. Eng. J.*, **2025**, *515*, 163453.
50. L. Wang; Z. Wang; S. K. Patel; S. Lin; M. Elimelech; *ACS Nano*, **2021**, *15*, 4093–4107.
51. M. Macha; S. Marion; V. V. R. Nandigana; A. Radenovic; *Nat. Rev. Mater.*, **2019**, *4*, 588.
52. M. Tsutsui; K. Yokota; I. W. Leong; Y. He; T. Kawai; *Cell Rep. Phys. Sci.*, **2022**, *3*, 101065.
53. K. Yazda; K. Bleau; Y. Zhang; X. Capaldi; T. St-Denis; P. Grutter; W. W. Reisner; *Nano Lett.*, **2021**, *21*, 4152–4159.
54. D. Brogioli; R. Ziano; R. A. Rica; D. Salerno; F. Mantegazza; J*. Colloid Interface Sci.*, **2013**, *407*, 457–466.
55. G. R. Iglesias ; S. Ahualli ; M. M. Fernandez ; M. L. Jimenez ; A. V. Delgado *J. Power Sources*, **2016**, *318*, 283–290.
56. M. Marino; L. Misuri; M. L. Jiménez; S. Ahualli; O. Kozynchenko; S. Tennison; M. Bryjak; D. Brogioli; *J. Colloid Interface Sci.*, **2014**, 436,146–153.

57. B. E. Conway, *Electrochemical Supercapacitors*, Kluver Academic, New York, **1999**.
58. B. B. Sales; M. Saakes; J. W. Post; C. J. N. Buisman; P. M. Biesheuvel; H. V. M. Hamelers; *Environ. Sci. Technol.*, **2010**, *44*, 5661–5665.
59. D. Lee; J. Choi; U. Paik; T. Song; Y. G. Jung; S. Yang; *Chem. Eng. J.*, **2025**, *525*, 170452.
60. Z. Zou; L. Liu; S. Meng; X. Bian; *Energy Rep*., **2022**, *8*, 7325–7335.
61. K. Smolinska-Kempisty; A. Siekierka; M. Bryjak; *Desalination*, **2020**, *482*,114384.
62. H. Choi; D. Kim; D. G. Kim; Y. Kim; J. G. Park; M. G. Kim; Y. G. Jung; J. Yoo; J. Baek; S. Kang; B. Kim; J. H. Bang; D. Lee; B. G. Kim; S. Yang; *Desalination*, **2024**, *581*, 117591.
63. H. Zhu; W. Xu; G. Tan; E. Whiddon; Y. Wang; C. G. Arges; X. Zhu; *Electrochim. Acta*, **2019**, *294*, 240-248.
64. S. Sarp; Z. Li; J. Saththasivama; *Desalination*, **2016**, *389*, 2-14.
65. https://www.power-technology.com/projects/statkraft-osmotic/ (accesat 15.05.2026)
66. https://www.renewableinstitute.org/japans-first-osmotic-power-plant-what-it-means-for-clean-energy/ (accesat 15.05.2026)